JOURNAL OF BACTERIOLOGY, Dec. 1986, p. 1430–1438
0021-9193/86/121430-09$02.00/0

Vol. 168, No. 3

Compartmentalization of the Periplasmic Space at Division Sites in Gram-Negative Bacteria

WILLIAM R. COOK,* THOMAS J. MACALISTER, AND LAWRENCE I. ROTHFIELD

Department of Microbiology, University of Connecticut Health Center, Farmington, Connecticut 06032

Received 22 July 1985/Accepted 23 September 1986

Phase-contrast and serial-section electron microscopy were used to study the patterns of localized plasmolysis that occur when cells of *Salmonella typhimurium* and *Escherichia coli* are exposed to hypertonic solutions of sucrose. In dividing cells the nascent septum was flanked by localized regions of periseptal plasmolysis. In randomly growing populations, plasmolysis bays that were not associated with septal ingrowth were clustered at the midpoint of the cell and at 1/4 and 3/4 cell lengths. The localized regions of plasmolysis were limited by continuous zones of adhesion that resembled the periseptal annular adhesion zones described previously in *lkyD* mutants of *S. typhimurium* (T. J. MacAlister, B. MacDonald, and L. I. Rothfield, Proc. Natl. Acad. Sci. USA 80:1372–1376, 1983). When cell division was blocked by growing *divC*(Ts) cells at elevated temperatures, the localized regions of plasmolysis were clustered along the aseptate filaments at positions that corresponded to sites where septum formation occurred when cell division was permitted to resume by a shift back to the permissive temperature. Taken together the results are consistent with a model in which extended zones of adhesion define localized compartments within the periplasmic space, predominantly located at future sites of cell division.

When gram-negative bacteria are plasmolyzed by exposure to hypertonic solutions of sucrose, the cytoplasmic membrane retracts from the rigid murein-outer membrane layer. This results in an expansion of periplasmic volume, leading to the formation of periplasmic bays that can be visualized in phase-contrast and electron micrographs (5, 12, 14, 15).

Bayer (2) has shown that discrete zones of adhesion between inner membrane, murein, and outer membrane can be visualized in electron micrographs of plasmolyzed cells. The adhesion zones presumably reflect specific murein-inner membrane attachments that resist the inward pull imposed by the osmotic stress.

Recently, MacAlister et al. (10) demonstrated the presence of annular murein-membrane attachments at sites of cell division in serial-section electron micrographs. The location of the periseptal annuli on either side of the aberrant division septa in a *lkyD* cell division mutant of *Salmonella typhimurium* suggested that the annuli might function by segregating the site of septation from the remainder of the cell envelope. It was suggested that the division septa of wild-type cells were also associated with periseptal annuli, although these were not clearly visualized when standard plasmolysis conditions were used. Similar structures have been reported to be present in *Escherichia coli* (1).

In this report we (i) define optimal conditions for visualizing the localized regions of plasmolysis that are associated with the annular attachment sites, (ii) confirm the presence of annular adhesion zones at septal and nonseptal locations in wild-type cells, (iii) show that these structures are located in topologically defined regions of the cell envelope that appear to correspond to future sites of cell division, and (iv) present evidence that the cell division block in *divC* mutants of *S. typhimurium* occurs after the stage of formation and localization of the annular attachment at potential division sites.

* Corresponding author.

MATERIALS AND METHODS

Strains. *E. coli* ML30 was obtained from F. Kepes, Institut Jacques Monod, Paris; *S. typhimurium* SA534 (*serA rfa-3058*) was obtained from K. Sanderson, University of Calgary, Calgary, Alberta, Canada. *S. typhimurium* TK484 [*divC*(Ts) *hisBHAFIE612 thy-1151*] was provided by Z. Ciesla (3). The *divC* mutation of *S. typhimurium* has also been called *envA* (13); however, because the electron microscopic appearance of strain TK484 grown at 42°C resembles that of *E. coli fts* mutants and does not resemble that of *E. coli envA* mutants (11), it appears desirable to retain the *divC* nomenclature until the relationships between the *E. coli* and *S. typhimurium* cell division genes are further clarified.

Bacterial growth and plasmolysis. Cells were grown in minimal medium consisting of M9 (4) containing 0.4% D-glucose, 50 μg of a general amino acid mixture per ml, and 0.05 μg of a general vitamin mixture and other required nutrients per ml, unless otherwise noted. Cultures were harvested during the mid-exponential phase of growth (optical density at 600 nm, 0.4 to 0.6) by centrifugation at 2,000 × *g* for 10 min at 5°C. The pellet was suspended in 0.1 volume of fresh culture medium at room temperature (21 to 23°C), and the suspended cells were plasmolyzed by adding an equal volume of plasmolyzing solution (0 to 77.2% sucrose [wt/vol], 10 M HEPES [*N*-2-hydroxyethylpiperazine-*N*′-2-ethanesulfonic acid pH 7.4]); in the remainder of this report, the sucrose concentrations used for plasmolysis are reported as final concentrations (0 to 38.6% [wt/vol]). After the cells were kept at room temperature for 3 min, they were fixed by the addition of glutaraldehyde to a final concentration of 2.5%. The suspension was allowed to stand for an additional 60 min at room temperature and centrifuged for 4 min at 14,000 × *g*, and the pellet was suspended in fresh medium (refractive index, 1.335).

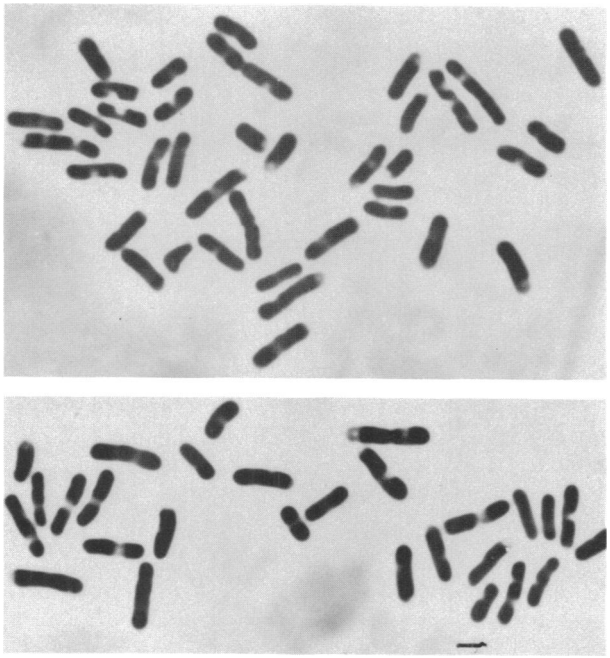

FIG. 1. Phase micrograph of plasmolyzed cells. An actively growing culture of *S. typhimurium* SA534 at 30°C was plasmolyzed in 13% sucrose. Plasmolysis bays are visible as the light areas within the cells and at the cell poles. Bar, 1 μm.

Analysis of plasmolyzed cells. Micrographs (Fig. 1) were taken with a phase-contrast microscope (BH-2; Olympus) (SPlan 100 PL objective) and a 35-mm camera (PM-10; Olympus). Cells in enlarged photographs (×2,900 total magnification) were analyzed with a computer-assisted digitization system and an electronic digitizing tablet (Bit-Pad-One; Summagraphics). All cells that were in sharp focus were analyzed. Cell lengths and bay positions were measured by tracing a cursor along the central axis of the cell. Positions of plasmolysis bays and septa were determined as described in the legend to Fig. 2.

To determine the experimental variability in measurement of cell lengths and bay positions, a set of cells containing combinations of polar plasmolysis bays, internal plasmolysis bays, and septa in frequencies that approximated those of the total population was repetitively digitized at three independent sessions for a total of 24 cycles of measurement. The average coefficients of variation of cell length measurement over the cell length range from 0.88 to 5.26 μm were 4.01% for cells containing no polar bays and 4.42% for cells containing one or two polar bays; 95% confidence limits were ±0.058 and ±0.061 μm, respectively, for the two groups of cells. The average coefficient of variation of measurement of internal bay positions was 4.47%. This resulted in a 95% confidence limit of ±0.062 μm, corresponding to ±0.094 cell lengths in the shortest cells and ±0.016 cell lengths in the longest cells in the population.

To determine whether a problem existed in discriminating between septa and bays in plasmolyzed cells, numbers of septa were determined in parallel samples of plasmolyzed and unplasmolyzed cells. In the unplasmolyzed sample, 76 septa were observed in 394 cells (0.19 septum per cell), whereas the plasmolyzed sample contained 68 septa in 407 cells (0.17 septum per cell). The similarity of these results suggests that confusion between bays and septa in the plasmolyzed samples is not a significant problem.

Other procedures. Electron microscopy was performed on random thin sections and on serial sections mounted on Formvar-backed, carbon-coated, slotted grids (10). The presence of the Formvar-carbon support that underlies the sections results in some loss of resolution and contrast but makes it possible to follow the same structure in a sufficient number of consecutive sections to define its long-range organization within a single cell. Cell volume analysis was performed with an electronic particle counter (30-μm aperture; 50-μl manometer; aperture current setting, 1/2; amplification setting, 1/4; model B; Coulter Electronics, Inc., Hialeah, Fla.) and a multichannel analyzer (model C-1000; Coulter). Prior to analysis, the fixed, plasmolyzed cells were diluted to approximately 8×10^5 cells per ml in 3.0% sodium chloride containing 0.01 M sodium azide. The particle volume determined in this way reflects the volume that is impermeant to the NaCl used in the diluent (9). Because NaCl freely crosses the outer membrane of gram-negative organisms, the particle volume therefore reflects the cytoplasmic volume of the suspended cells.

RESULTS

Phase-contrast microscopy of plasmolyzed cells. When cells were viewed by phase-contrast microscopy after exposure to hypertonic sucrose, plasmolysis bays were visible as clear areas at the poles, along the length of the cell, or both (Fig. 1). Phase-contrast micrographs of cells from control preparations, in which sucrose was omitted from the plasmolyzing solution, did not show plasmolysis bays or other internal inclusions. This is consistent with the previous demonstration (16) that nucleoids cannot be visualized in phase-contrast micrographs of glutaraldehyde-fixed cells sus-

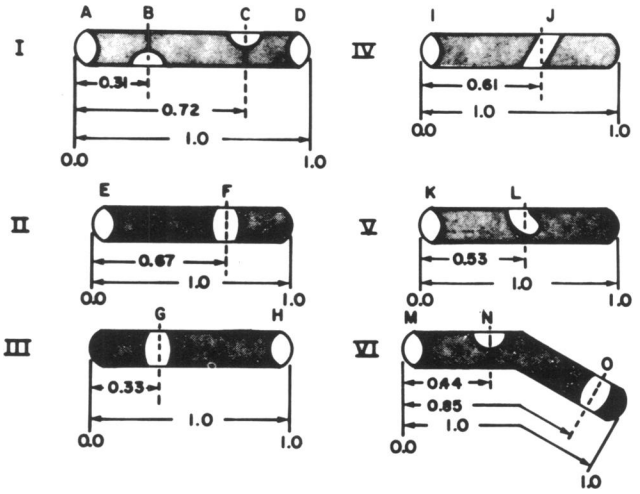

FIG. 2. Method of determining the position of plasmolysis bays in phase-contrast micrographs of plasmolyzed cells. The positions of plasmolysis bays along the long axis of the cell were defined by visually identifying the apparent optical center of the bay (broken lines; individual bays are indicated by capital letters) and extending this point through the central axis of the cell. The distance of each bay from the cell pole was expressed as a fraction of the total cell length. Plasmolysis bays at the ends of cells were assigned to the poles (positions 0.0 and 1.0 cell length). Because the pole used as the origin was chosen randomly, cells II and III are equivalent (i.e., bays F and G were randomly assigned a position at either 0.33 or 0.67 cell length). The positions of septal constrictions were determined in a similar manner.

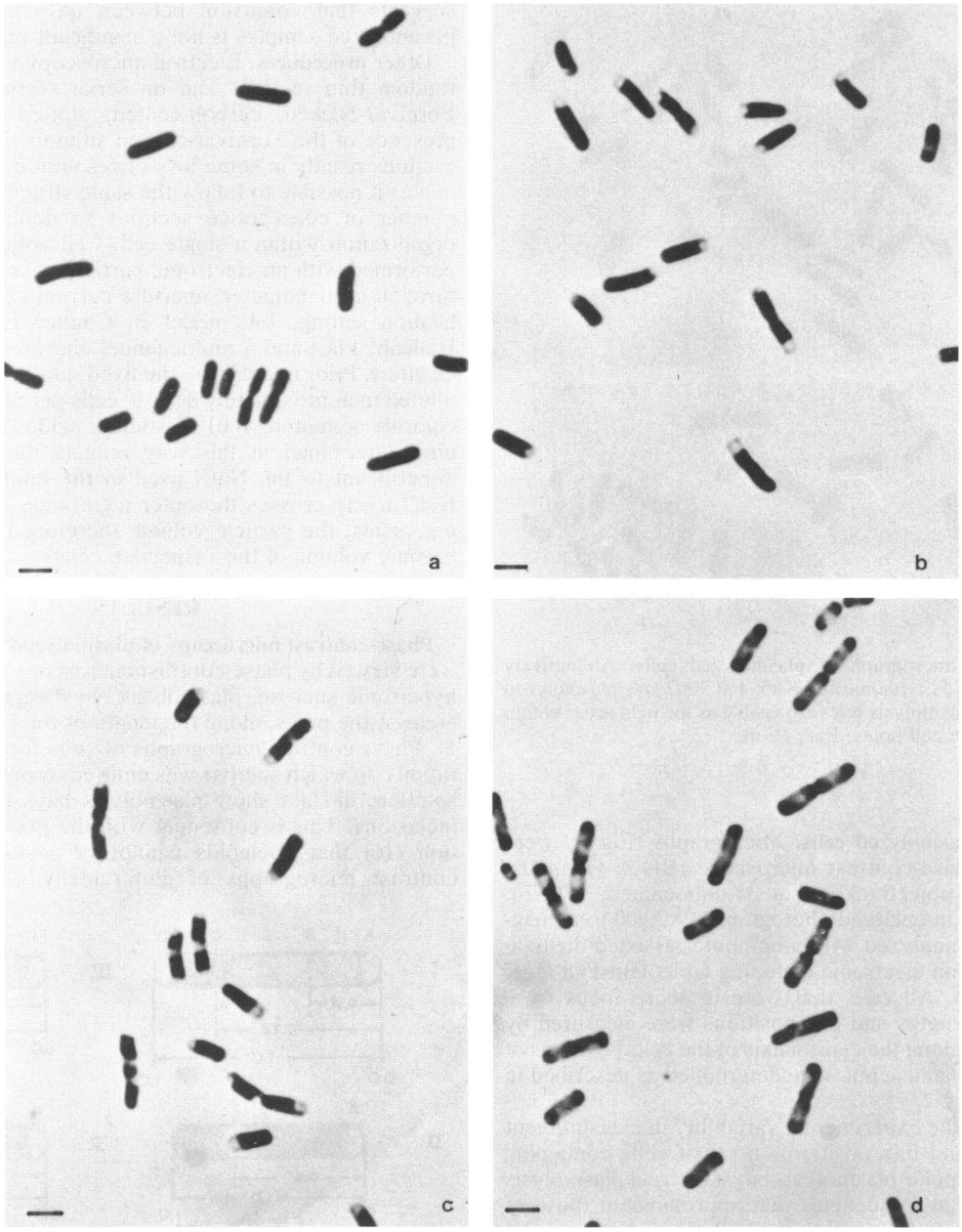

FIG. 3. Phase-contrast micrographs of cells of *S. typhimurium* SA534 plasmolyzed in 0% (a), 19% (b), 26% (c), and 35% (d) sucrose concentrations. Cells were grown as described in footnote *a* of Table 1. Bars, 1 μm.

pended in medium with a refractive index below 1.401 and argues against the possibility that plasmolysis bays and nucleoids were confused in this analysis. As described below, each plasmolysis bay represented a region of localized expansion of the periplasmic space. Maximal numbers of clearly defined internal plasmolysis bays were seen after 3 min of exposure to the plasmolyzing medium at 22°C. Longer times of exposure resulted in reversal of the plasmolysis, as shown by disappearance of the bays. Therefore, in all subsequent experiments cells were exposed to the plasmolyzing medium for 3 min, followed by glutaraldehyde fixation to preserve the plasmolysis pattern.

To determine the effect of sucrose concentration on the plasmolysis pattern, cells were examined after plasmolysis in various sucrose concentrations (0 to 39% final concentrations). This revealed a progressive increase in the number of visible plasmolysis bays as the sucrose concentration was increased. The number of bays reached a maximum at intermediate sucrose concentrations, with a dramatic decrease in visible bays when higher concentrations were used (Table 1). The sucrose concentration that gave maximum numbers of internal bays varied, depending on strain and growth conditions, as described below.

The pattern of distribution of plasmolysis bays along the length of the cell also varied with sucrose concentration (Table 1 and Fig. 3). At low concentrations most of the visible bays were located at the cell poles, whereas the number of internal bays increased when intermediate con-

TABLE 1. Number and location of plasmolysis bays as a function of sucrose concentration[a]

Sucrose concn (%; wt/vol)	No. of cells	No. of bays/cell	No. of the following/cell:		Median cell vol (μm^3)
			Internal bays	Polar bays	
13	161	<0.01	<0.01	<0.01	0.672
16	99	0.02	0.02	<0.01	ND[b]
19	129	0.59	0.22	0.36	0.648
23	150	1.01	0.45	0.55	ND
26	110	1.74	1.24	0.50	0.624
29	96	1.88	1.53	0.34	ND
32	91	1.37	1.13	0.24	0.600
35	115	0.88	0.74	0.14	ND
39	138	0.07	0.06	0.14	0.576

[a] S. typhimurium SA534 was grown at 37°C in proteose peptone-beef extract medium (Difco Laboratories, Detroit, Mich.) prior to plasmolysis and examination by phase-contrast microscopy.
[b] ND, Not determined.

centrations were used, as described previously by Scheie (14) for *E. coli* B/r. At high sucrose concentrations there were fewer polar bays and there was a broadening and loss of definition of the internal bays. At the highest concentrations plasmolysis was extensive, and discrete plasmolysis bays were not observed. The loss of discrete internal bays at the higher sucrose concentrations suggests that the large pressure differential associated with the higher external sucrose concentrations was capable of breaking inner membrane-murein attachments that were resistant to disruption under milder conditions of plasmolysis.

Maximum numbers of well-defined plasmolysis bays were observed within a relatively narrow range of sucrose concentrations that varied from organism to organism and also varied according to growth conditions. Lower sucrose concentrations were required for cells in the late exponential growth phase than for cells in the early exponential growth phase, and in stationary-phase cultures some cells showed spontaneous plasmolysis even in the absence of sucrose. In addition, cells grown in media with high osmotic strengths required higher concentrations of sucrose for optimal plasmolysis than cells grown in media with low osmotic strengths. For each strain and growth condition, preliminary experiments were performed to determine the concentration of sucrose that produced the maximum number of clearly defined internal bays (Fig. 1). This concentration was then used to induce plasmolysis in the experimental samples.

In phase-contrast micrographs of optimally plasmolyzed cells, the internal plasmolysis bays varied in appearance in different cells, falling roughly into four classes (Fig. 4). In the most prevalent classes (classes I and II), which accounted for approximately 90% of internal bays, bays were oriented at right angles to the long axis of the cell and extended either completely or partially across the width of the cylinder. Class III bays appeared as diagonal structures that extended across the width of the cell. Class IV bays extended inward from one side of the cell profile and were asymmetrically oriented relative to the long axis of the cell.

Electron microscopy of plasmolyzed cells. Three types of plasmolysis bays could be distinguished (Fig. 5 to 7). (i) Plasmolysis bays were frequently present at the poles of the cells, corresponding to the polar bays present in phase-contrast micrographs. Serial-section electron microscopy (data not shown) confirmed that each polar plasmolysis bay was bounded by an anular adhesion zone, as described previously (10). (ii) In septating cells regions of localized plasmolysis were present on either side of the nascent

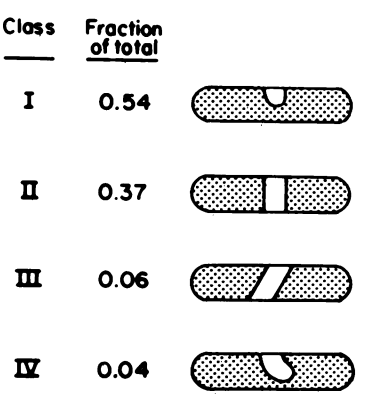

FIG. 4. Classes of internal plasmolysis bays. The frequency of occurrence of each class of internal bay (expressed as fraction of the total number of internal bays) was determined in cells of *S. typhimurium* SA534 plasmolyzed in 13% sucrose (Fig. 1) from analysis of 407 randomly selected cells containing 345 internal plasmolysis bays.

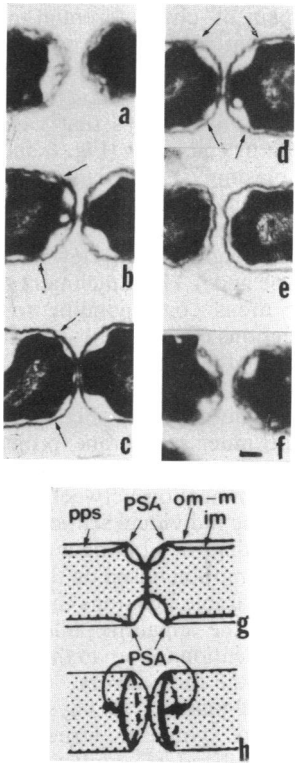

FIG. 5. Septal region of a plasmolyzed cell of *S. typhimurium* SA534. (a to f) Serial sections through the septal region of a dividing cell showing localized regions of plasmolysis flanking the nascent septum; arrows indicate the attachment sites that form the periseptal annuli. Bar, 0.1 μm. (g) Diagrammatic representation of the central section of the serial micrographs. Abbreviations: im, inner membrane; om-m, outer membrane-murein layer; pps, periplasmic space; PSA, periseptal annuli. (h) Surface reconstruction of the borders of the localized regions of plasmolysis in the serial micrographs. Arrows indicate the positions of the attachment sites that limit the regions of localized plasmolysis.

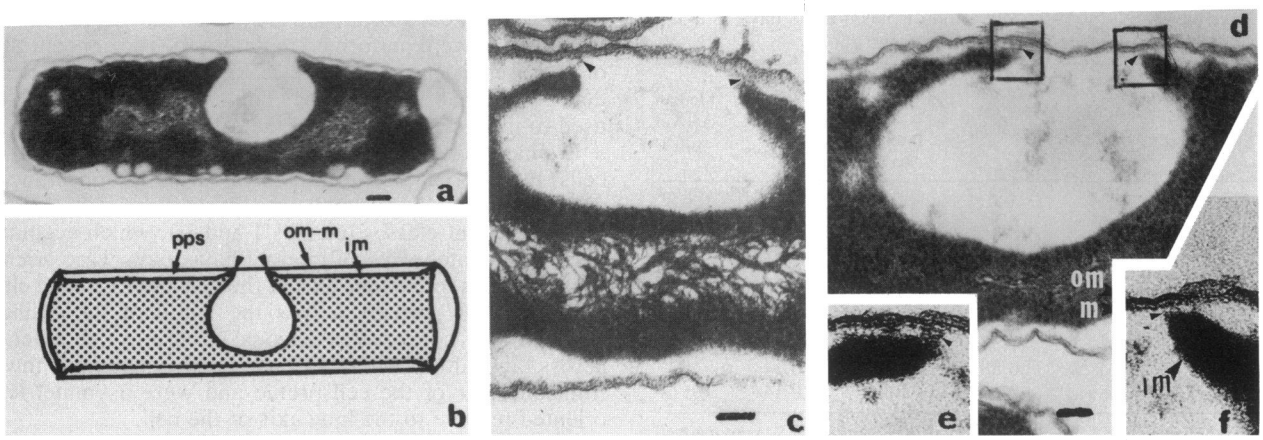

FIG. 6. Electron micrograph of a plasmolyzed cell of *S. typhimurium* SA534. (a) A nondividing cell containing a single internal plasmolysis bay and a polar plasmolysis bay. Bar, 0.1 μm. (b) Diagrammatic representation of the section (adapted from previously published data [8]). Arrows indicate the positions of the attachment sites that limit the regions of local plasmolysis. Abbreviations are defined in the legend to Fig. 5. (c, d) Random sections through localized regions of plasmolysis. A portion of the nucleoid is visible below the plasmolysis bay shown in panel c. Arrowheads indicate the positions of adhesion sites that appear to form the lateral limits of the plasmolysis bays. Bars, 0.1 μm. (e and f) Higher power views of attachment sites. The regions enclosed in the boxes in panel d were enlarged 2.5-fold. The photographs have been overexposed to enhance the attachment sites (indicated by the unlabeled arrowheads). Abbreviations: om, outer membrane; m, murein layer; im, inner membrane.

septum (Fig. 5). Each periseptal plasmolysis bay was bounded by a pair of circumferential membrane-murein attachment zones that flanked the nascent septum, corresponding to the periseptal anuli that were previously shown to flank the incomplete septa of *lkyD* (10). (iii) Many cells also contained plasmolysis bays that were not associated with division septa or cell poles (Fig. 6 and 7).

The nonseptal plasmolysis bays appeared to be limited by sites where the inner membrane was closely associated with the inner surface of the murein-outer membrane layer. Characteristic high-magnification views of these structures are shown in Fig. 6e and f. The attachment sites were usually flanked by clear areas corresponding to the periplasmic space. In serial sections of some cells, the attachments could be followed through the complete series of sections as a narrow structure located between the inner membrane and the murein-outer membrane layer (Fig. 7a). In serial sections of other cells, the inner membrane projected toward the outer layers at corresponding sites in all sections, although the electron-dense connection between the layers was visible in only some of the individual sections (Fig. 7b and c). In these cases the idea that the limiting attachment zones were continuous is a presumption based on the presence of visible attachments at comparable locations in the flanking sections of the series and on the apparent pulling outward of inner membrane at these locations, even in the absence of a visible connection between the three layers.

Most of the internal plasmolysis bays that were examined in serial sections were symmetric structures (Fig. 6 and 7). These regions of localized plasmolysis presumably corresponded to the class I and II bays seen in phase-contrast micrographs (Fig. 4). In occasional cases the zones of local plasmolysis ran obliquely at an angle to the long axis of the cylinder, presumably corresponding to class III and IV bays, and more complex structures also were sometimes seen. The circumferential murein-membrane attachments that defined the nonseptal plasmolysis bays were generally oriented perpendicular to the long axis of the cell (Fig. 7), but they often extended only partly around the cylinder (Fig. 7d to f). A more detailed description of the three-dimensional structure of the continuous attachment sites will be published separately.

Localization of plasmolysis bays along the long axis of the cell. To determine whether the localized periplasmic compartments showed a characteristic pattern of localization within the cell, we analyzed the distribution of plasmolysis bays in phase-contrast micrographs of large numbers of actively growing cells.

Because phase-contrast micrographs represent two-dimensional projections of three-dimensional structures, the apparent location of an asymmetric plamolysis bay along the long axis may be affected by the rotational orientation of the cell. This is particularly true for the relatively small number of cells containing asymmetric bays (classes III and IV in Fig. 4) but cannot be excluded for other classes as well. In this study we assumed that the analysis of large numbers of cells provided a random sampling of the possible rotational orientations, thereby giving a valid description of the average positions of bays in the overall population. The validity of this assumption is discussed further below.

Analysis of the distribution of plasmolysis bays in cells of *S. typhimurium* and *E. coli* revealed that the internal bays were not randomly distributed but were clustered in three locations along the length of the cell (Fig. 8). A major peak was present at the midpoint of the cell, which is consistent with the previous suggestion that periseptal anuli are formed at sites of cell division prior to the onset of septal invagination. In addition, however, two smaller peaks were present at 1/4 and 3/4 cell lengths, sites that presumably would be used for septum formation during the next division cycle. Similar results were obtained with cultures of *S. typhimurium* SA534 grown with generation times of 73 min (Fig. 8A) and 104 min, cultures of *E. coli* ML30 grown with a generation time of 55 min (Fig. 8B), and several other strains of *E. coli* K-12 and *S. typhimurium* grown under similar conditions.

We considered several possible artifacts that might explain the clustering at 1/4, 1/2, and 3/4 cell lengths.

The results do not appear to reflect irreproducibility of the measuring technique, as shown by the low coefficient of

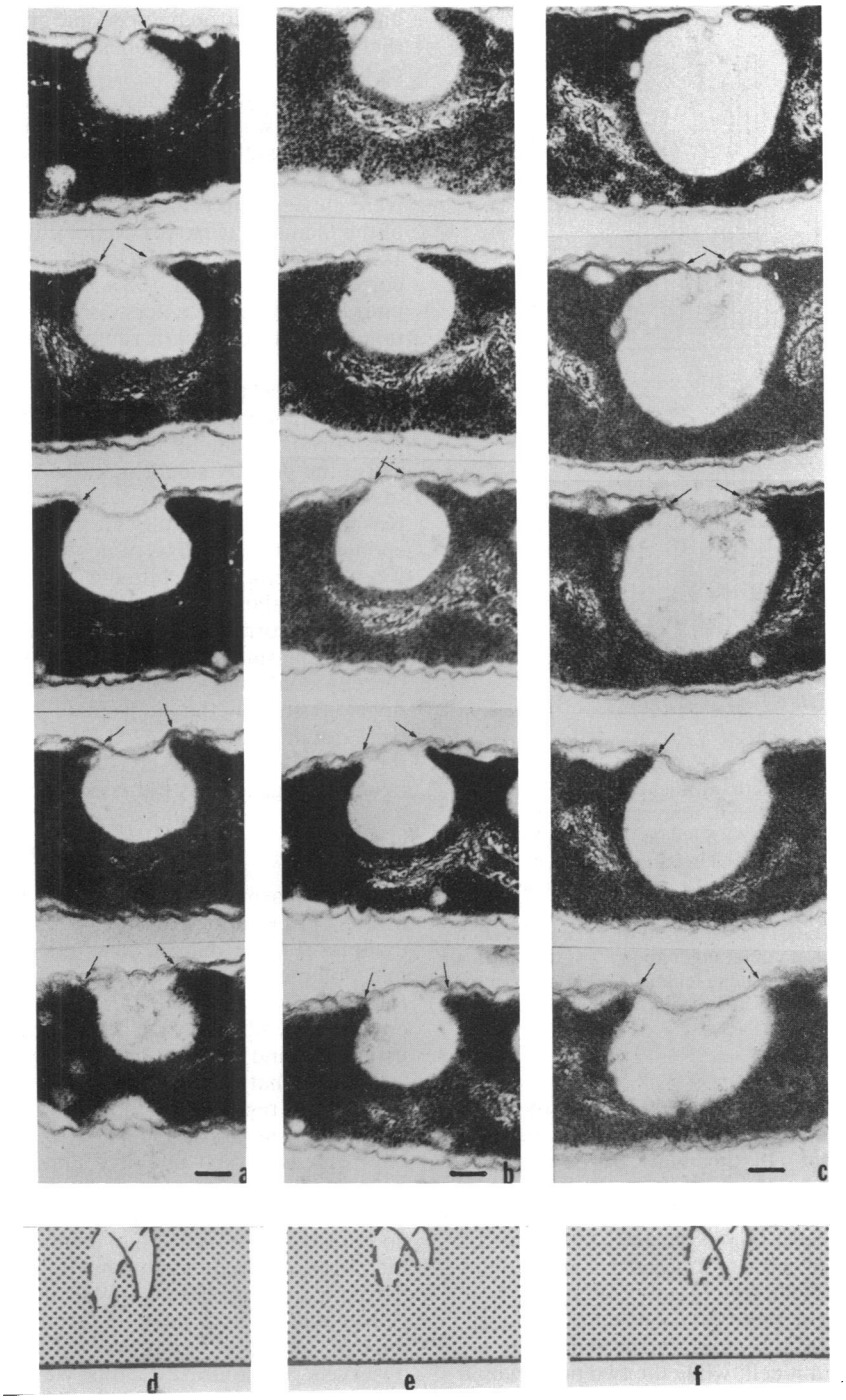

FIG. 7. Serial sections of nonseptal plasmolysis bays in cells of *S. typhimurium* SA534. (a to c) Serial sections of typical plasmolysis bays in *S. typhimurium* SA534. a, b, and c each represent serial sections through an internal plasmolysis bay within an individual cell. Arrows indicate the positions of visible attachments that limit the region of plasmolysis. The cytoplasmic membrane projects toward the cell surface at the site of the visible attachments. There is a similar abrupt angling of cytoplasmic membrane toward the outer layers at corresponding locations in sections in which there is no visible electron-dense material between the cell envelope layers. Bars, 0.1 μm. (d to f) Surface reconstructions of the borders of the localized plasmolysis bays shown in columns a, b, and c, respectively.

variation of measurement (see above) and the similarity of the distribution pattern in different strains and with the same strain in different experiments. Similarly, the clustered distribution and the reproducibility of the patterns support the assumption that a sufficient number of cells was examined to exclude biases due to inadequate sampling of the possible rotational orientations of asymmetric bays.

We also considered the possibility that the circumferential membrane-murein adhesion zones that attach bays to the cell envelope might be randomly distributed along the length

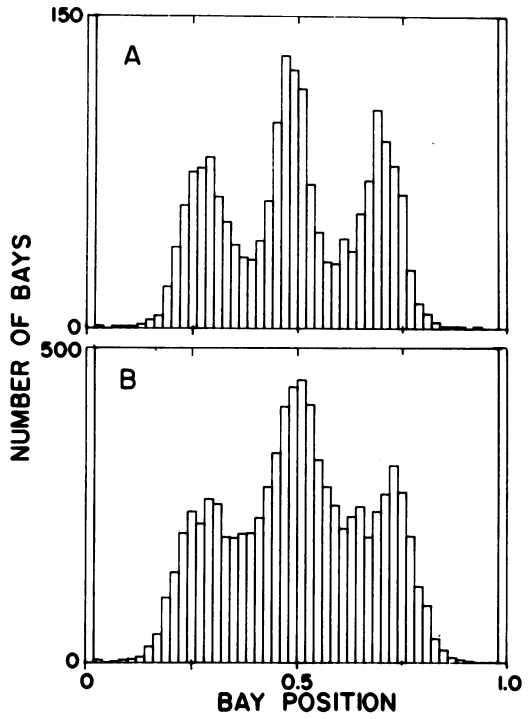

FIG. 8. Distribution of plasmolysis bays along the length of plasmolyzed cells of *S. typhimurium* and *E. coli*. The horizontal axis represents position along the length of the cell, determined as described in the text. The vertical axis represents the number of plasmolysis bays at each position. (A) *S. typhimurium* SA534 was plasmolyzed in 13% sucrose after growth in minimal medium at 30°C (generation time, 73 min). A total of 2,029 cells (mean length, 3.0 μm) containing 3.453 plasmolysis bays were examined; 1,475 of the bays were located at the poles. (B) *E. coli* ML30 was plasmolyzed in 23.5% sucrose after growth in minimal medium at 37°C (generation time, 55 min). A total of 9,344 cells (mean length, 2.6 μm) containing 15,084 bays were examined; 6,885 of the bays were located at the poles.

of the cell, despite the fact that the centers of the bays themselves were clustered at 1/4, 1/2, and 3/4 cell lengths in phase-contrast micrographs. In this view bays that originated from attachments near the ends of the cell might be constrained in their ability to expand laterally because of the presence of the cell pole, resulting in clustering at about 1/2 cell length. The clusters of bays at 1/4 and 3/4 cell lengths could be explained in a similar way if cells containing these lateral bays also contained nascent division septa at midcell. In this case the incomplete septum might constrain the expansion of bays toward midcell, while the two poles would constrain expansion toward the cell ends. This could result in clustering at 1/4 and 3/4 cell lengths.

Evidence that the clustering of plasmolysis bays at putative division sites is not caused by constraints due to the proximity of cell poles and septa is presented in the following section, in which it is shown that plasmolysis bays are also located at potential division sites in the nonseptate filaments of certain cell division mutants.

Periplasmic compartmentalization in *divC* mutants. As described previously (3, 6), growth of *S. typhimurium* TK484 [*divC*(Ts)] cells at elevated temperatures results in formation of long filaments that contain no visible septa (Fig. 9a and f). When these cells were plasmolyzed, multiple plasmolysis bays were visible along the length of the filaments (Fig. 9b and d). The electron microscopic appearance of the bays and their limiting adhesion zones was similar to that of wild-type cells.

Evidence that the plasmolysis bays were nonrandomly distributed was obtained by analyzing their distribution along the length of the filaments in cells grown at 42°C for approximately two generations. This revealed that the bays were clustered in peaks at regular intervals along the length of the filaments (Fig. 10). Major clusters were located at 1/4, 1/2, and 3/4 cell lengths with smaller peaks at locations corresponding to 1/8, 3/8, 5/8, and 7/8 cell lengths. The intervals between clusters corresponded to a constant fraction of total cell length rather than to a constant absolute distance.

The regularity of the distribution pattern suggested that the attachment sites that limited the localized regions of plasmolysis might be located at future division sites. Because the cell division block due to the *divC* mutation was reversible (Fig. 9c and e), we asked whether the locations of plasmolysis bays in the filaments formed at 42°C corresponded to the positions of new septa that were later formed when the cells were shifted back to 30°C. The locations of new septa along the filaments 20 min after the shiftdown (Fig. 10b) corresponded to the previously observed major peaks of plasmolysis bays prior to the shiftdown (Fig. 10a), thereby confirming that the bays were located at potential division sites in the nonseptate filaments. Because septa were not present in the 42°C filaments, the observed clustering of bays at potential division sites could not have resulted from topological constraints imposed by septa and cell poles.

DISCUSSION

During plasmolysis the presence of a nonpermeant solute in the periplasmic space causes movement of water from cytoplasm to periplasm, resulting in an increased periplasmic volume. It has long been known that this results in formation of localized regions of plasmolysis within the cell envelope (5, 12, 14, 15). This was confirmed in this study by using light and electron microscopy.

The fact that expansion of the periplasmic space is limited to localized regions is incompatible with a model that views the periplasm as an open aqueous compartment that is interrupted only by a limited number of punctate zones of adhesion that attach inner membrane to the murein-outer membrane layer (2). According to this model there should be no barrier to the lateral movement of periplasmic water. In the absence of extended zones of adhesion or other similar barriers, the increased periplasmic volume of plasmolyzed cells would be distributed uniformly around the periphery of the cell, and localized regions of plasmolysis would not be observed. In contrast to this view, the fact that discrete plasmolysis bays occur in defined locations along the body of the cell implies that the cell envelope contains localized periplasmic compartments.

The relationship between the punctate zones of adhesion described by Bayer (2) and the murein-membrane attachment sites that appear to form the boundaries of the localized plasmolysis bays has not been established. It is not known whether they represent different aspects of the same basic structure or whether they reflect two different types of membrane-murein attachment that are topologically and functionally distinct.

Although the continuous attachment zones in nonseptal regions appeared to sequester localized regions of plasmolysis, they did not extend completely around the circum-

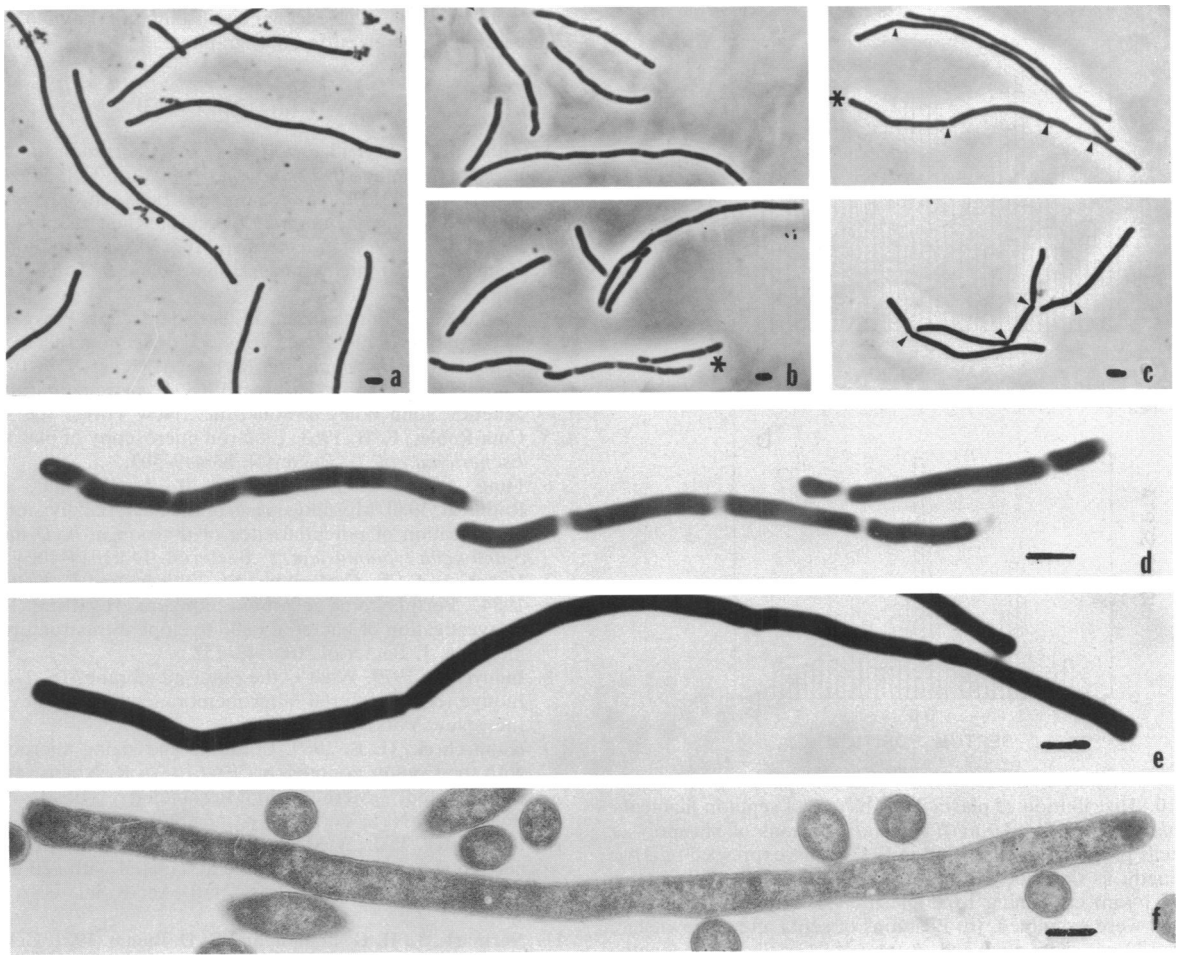

FIG. 9. Micrographs of cells of *S. typhimurium* TK484 [*divC*(Ts)]. (a) Actively growing cells at 30°C (optical density at 600 nm, 0.25) were shifted to 42°C for 120 min. Bar, 1.0 μm. (b) Unplasmolyzed cells were fixed with glutaraldehyde and prepared for phase-contrast and electron microscopy, as described in the text. (b) A portion of the culture (panel a) was plasmolyzed in 13% sucrose and prepared for phase-contrast microscopy. Plasmolysis bays are visible along the length of the filaments. The asterisk indicates the group of cells that are enlarged in panel d. Bar, 1.0 μm. (c) A portion of the culture (panel a) was diluted in fresh prewarmed medium to an optical density at 600 nm of 0.1 and was then shifted to 30°C. After 20 min growth was stopped by the addition of glutaraldehyde to a final concentration of 2.5%, and unplasmolyzed cells were prepared for phase-contrast microscopy. Arrowheads indicate the locations of septa along the filament. The asterisk indicates the cell that is enlarged in panel e. Bar, 1.0 μm. (d and e) Enlargements of cells indicated by asterisks in panels b and c, respectively. Bar, 1 μm. (f) Electron micrograph of filaments after growth for 120 min at 42°C. No septa are visible. Bar, 0.5 μm.

ference of the cell (Fig. 7). They may represent early stages in the development of mature periseptal annuli (10), but verification of this hypothesis will require more direct evidence for the suggested biogenetic relationship between the nonseptal and septal attachment zones. The presence of localized plasmolysis bays could also reflect the presence of large numbers of closely spaced adhesion zones in other regions of the cell envelope, local differences in the suggested gel-like organization of the periplasm (7), or the existence in nonplasmolyzed regions of different types of murein-inner membrane association that are more resistant to disruption by the plasmolysis procedure.

An unexpected finding of this study was the clustering of periplasmic bays at 1/4 and 3/4 cell lengths in wild-type cells. We suggest that these reflect the presence of nascent annuli at these sites that are precursors of the periseptal annuli that will participate in the septation process during the next division cycle. In this view the structures at 1/4 and 3/4 cell lengths would be retained as periseptal annuli at the midpoints of the two daughter cells. If correct, this implies that the division site can be identified and can undergo the initial stages of its differentiation prior to the cell cycle in which it is used for septum formation. The results of this study were obtained from random populations of unsynchronized cells and therefore represent average values for cells at all stages of development. A test of the model will require studies of cells at different stages of progression through the division cycle, and a decision regarding its validity must await these results.

The demonstration that aseptate DivC$^-$ filaments contain annular adhesion zones at sites that are used for septum formation when the cells are returned to the permissive temperature indicates that these sites were already identified and committed to the division process dring the period of growth at 42°C. We conclude (i) that the adhesion zones that define the limits of plasmolysis bays in *divC* filaments are located at potential division sites; (ii) that the annuli and other division components at these sites are competent to

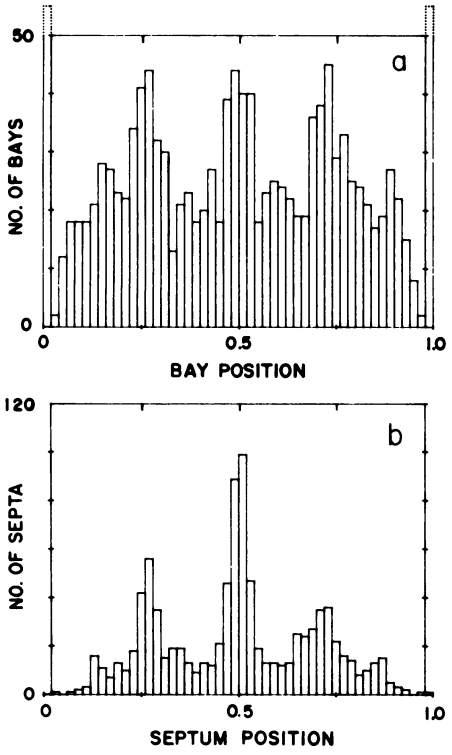

FIG. 10. Distribution of plasmolysis bays and septa in filaments of *S. typhimurium* TK484 [*divC*(Ts)]. (a) Positions of plasmolysis bays in cells prepared as described in Fig. 9b are expressed relative to cell length, as described in the text. A total of 381 cells (mean length, 17.1 μm) containing 1,695 plasmolysis bays (including 480 polar bays) were examined. (b) Positions of septa after a downshift to 30°C for 20 min were analyzed. A total of 943 cells (mean length, 25.1 μm) containing 1,443 septa were examined.

support septal morphogenesis when the function of the *divC* gene product is restored by return to the permissive temperature; and therefore, (iii) that the *divC* gene product acts after the stages of biogenesis, maturation, and localization of the periseptal annuli but before the stage of initiation of septal invagination. This lends support to the idea that formation and localization of periseptal annuli precedes the onset of septal invagination during the course of the division cycle.

ACKNOWLEDGMENTS

This study was supported by grant PCM 82-03516 from the National Science Foundation and Public Health Service grant AI-22183 from the National Institutes of Health.

We acknowledge the excellent assistance of Lavinia Muncy in preparation of the electron micrographs.

LITERATURE CITED

1. **Anba, J., A. Bernadac, J. Pages, and C. Lazdunski.** 1984. The periseptal annulus in *Escherichia coli*. Biol. Cell **50**:273–278.
2. **Bayer, M. E.** 1979. The fusion sites between outer membrane and cytoplasmic membrane of bacteria: their role in membrane assembly and virus infection, p. 167–202. *In* M. Inouye (ed.), Bacterial outer membranes. John Wiley & Sons, Inc., New York.
3. **Ciesla, Z., M. Badgasarian, W. Szerkiewicz, M. Przygonska, and T. Klopotowski.** 1972. Defective cell division in thermosensitive mutants of *S. typhimurium*. Mol. Gen. Genet. **116**:107–125.
4. **Clowes, R. C., and W. Hayes.** 1968. Experiments in molecular genetics. John Wiley & Sons, Inc., New York.
5. **Cota-Robles, E. H.** 1963. Electron microscopy of plasmolysis in *Escherichia coli*. J. Bacteriol. **85**:449–503.
6. **Fung, J. C., T. J. MacAlister, R. A. Weigand, and L. I. Rothfield.** 1980. Morphogenesis of the bacterial division septum: identification of potential sites of division in *lkyD* mutants of *Salmonella typhimurium*. J. Bacteriol. **143**:1019–1024.
7. **Hobot, J. A., E. Carlemalm, W. Villiger, and E. Kellenberger.** 1984. Periplasmic gel: new concept resulting from the reinvestigation of bacterial cell envelope ultrastructure by new methods. J. Bacteriol. **160**:143–152.
8. **Inouye, M.** 1979. What is the outer membrane?, p. 1–12. *In* M. Inouye (ed.), Bacterial outer membranes. John Wiley & Sons, Inc., New York.
9. **Kubitscheck, H. E.** 1969. Counting and sizing microorganisms with the Coulter counter, p. 593–610. *In* R. Norris, and D. W. Ribbons (ed.), Methods in Microbiology, vol. 1. Academic Press, Inc., New York.
10. **MacAlister, T. J., B. MacDonald, and L. I. Rothfield.** 1983. The periseptal annulus: an organelle associated with cell division in gram-negative bacteria. Proc. Natl. Acad. Sci. USA **80**:1372–1376.
11. **Normark, S., H. G. Boman, and G. D. Bloom.** 1971. Cell division in a chain-forming *envA* mutant of *Escherichia coli*. Acta Pathol. Microbiol. Scand. Sect. B **79**:651–664.
12. **Olijhoek, A. J. M., C. G. Van Eden, F. J. Trueba, E. Pas, and N. Nanninga.** 1982. Plasmolysis during the division cycle of *Escherichia coli*. J. Bacteriol. **151**:479–483.
13. **Sanderson, K. E., and J. R. Roth.** 1983. Linkage map of *Salmonella typhimurium*, edition VI. Microbiol. Rev. **47**:410–453.
14. **Scheie, P. O.** 1969. Plasmolysis of *Escherichia coli* B/r with sucrose. J. Bacteriol. **98**:335–340.
15. **Scheie, P. O., and R. Rehberg.** 1972. Response of *Escherichia coli* B/r to high concentrations of sucrose in a nutrient medium. J. Bacteriol. **109**:229–235.
16. **Valkenburg, J. A. C., and C. L. Woldringh.** 1984. Phase separation between nucleoid and cytoplasm in *Escherichia coli* as defined by immersive refractometry. J. Bacteriol. **160**: 1151–1157.